

See discussions, stats, and author profiles for this publication at: <https://www.researchgate.net/publication/263821155>

Optical super resolution using a lattice of light spots

Conference Paper · June 2014

DOI: 10.1364/COSI.2014.CM2D.5

CITATIONS

0

READS

83

4 authors:



[Prasanna Rangarajan](#)

Southern Methodist University

26 PUBLICATIONS 129 CITATIONS

[SEE PROFILE](#)



[Indranil Sinharoy](#)

Southern Methodist University

13 PUBLICATIONS 13 CITATIONS

[SEE PROFILE](#)



[Marc Peter Christensen](#)

Southern Methodist University

131 PUBLICATIONS 723 CITATIONS

[SEE PROFILE](#)



[Predrag Milojkovic](#)

DARPA

49 PUBLICATIONS 307 CITATIONS

[SEE PROFILE](#)

Some of the authors of this publication are also working on these related projects:



OMNISCIENT [View project](#)



OSR at macroscopic scales [View project](#)

All content following this page was uploaded by [Prasanna Rangarajan](#) on 19 January 2015.

The user has requested enhancement of the downloaded file. All in-text references [underlined in blue](#) are added to the original document and are linked to publications on ResearchGate, letting you access and read them immediately.

Optical super resolution using a lattice of light spots

Prasanna Rangarajan, Indranil Sinharoy, Marc P. Christensen and Predrag Milojkovic²

Department of Electrical Engineering, Southern Methodist University, 6251 Airline Road, Dallas, TX 75275-0338

²*Army Research Laboratory, 2800 Powder Mill Road, Adelphi, MD 20783-1197*

prangara@smu.edu, isinharoy@smu.edu, mpc@hyle.smu.edu, predrag.milojkovic@arl.army.mil

Abstract: The paper outlines a super resolution strategy that overcomes the severe anisotropy in the resolving power of a single-lens imager, by processing images acquired under a lattice of light spots.

OCIS codes: (100.6640) Super-resolution; (110.1758) Computational Imaging;

1. Motivation

Optical super resolution in the macroscopic regime has not achieved the same level of success as super-resolution microscopy. Reasons include the presence of field dependent aberrations, and the potential for aliasing.

Previous work [1] by the authors has established that aberrations do not preclude the possibility of super resolution. The work has also confirmed that space-variance in the optical blur introduces ghost artifacts in the super-resolved image, and exaggerates the anisotropy in the resolving power of the engineered imager. The strategy discussed herein represents a first response to the aforementioned issues. It examines the prospect of engineering the point spread function (PSF) of a single-lens imager using a lattice of light spots. Our choice of the illumination pattern is motivated by the observation that its product with a field dependent PSF, resembles a damped pulse train whose central lobe width is independent of field position.

Literature on super-resolution is replete with techniques using lattice illumination. But these techniques employ expertly designed optics characterized by a space-invariant PSF. Further, the lattice spacing is chosen to avoid crosstalk between adjacent spots in the camera image. The super resolution strategy outlined below relaxes both constraints.

2. Proposed strategy

Our inquiry begins with an attempt to identify the relation between the scene radiance and image intensity in the apparatus of Figure 1. In the interest of simplicity and clarity, our analysis makes the following assumptions:

1. The imaging and illumination paths share a single viewpoint.
2. The relative magnification between the imaging and illumination paths is unity.
3. The illumination pattern $p(x, y)$ is expressible as a weighted combination of non-overlapping light-spots/pixels of size $\Delta \times \Delta \mu\text{m}$. The light distribution in each spot follows a top-hat distribution, so that

$$p(x, y) = \left(\sum_{k, \ell=-\infty}^{\infty} \psi[k, \ell] \delta(x - k\Delta, y - \ell\Delta) \right) \otimes \text{rect}\left(\frac{x}{\Delta}, \frac{y}{\Delta}\right) \quad \text{wherein } \text{rect}(x, y) \stackrel{\text{def}}{=} \begin{cases} 1, & |x|, |y| < 0.5 \\ 0.5, & |x|, |y| = 0.5 \\ 0, & \text{otherwise} \end{cases}$$

4. The illumination pattern has a periodicity of P & Q projector pixels in the horizontal and vertical directions, respectively. This implies that $\psi[k + P, \ell + Q] = \psi[k, \ell]$ for all $k, \ell, P, Q \in \mathbb{Z}^+$.

Bearing the above assumptions in mind, one may attempt to derive the expression for the camera image in the apparatus of Figure 1. The result disclosed in Eq.(1), follows the notation of Lohmann and Paris [2].

$$i(x, y) = \iint p(u, v) r(u, v) h_{\text{cam}}(x - u, y - v; u, v) dudv \quad (1)$$

$p(u, v) = \left(\sum_{k, \ell=-\infty}^{\infty} \delta(u - kP\Delta, v - \ell Q\Delta) \right) \otimes \text{rect}\left(\frac{u}{\Delta}, \frac{v}{\Delta}\right)$	lattice illumination pattern with a period of $P\Delta \times Q\Delta \mu\text{m}$ in the principal directions
$r(u, v)$	geometric image of scene
$h_{\text{cam}}(x, y; u, v)$	spatially varying PSF of the single-lens imager

Super resolution is predicated on the observation of unresolved spatial frequencies in the camera image $i(x, y)$. Fourier analysis of the product $p(u, v)r(u, v)$ in Eq.(1) confirms that modulation smears the object spectrum across the optical passband. The challenge lies in undoing the smearing induced by amplitude modulation. The proposed solution exploits the modulation diversity afforded by translating the illumination pattern $p(x, y)$, in integer increments of Δ . The super resolved image is assembled by demodulating the temporal sequence of images acquired under integer pixel translates of the lattice illumination pattern $p(x, y)$, and accumulating the result. The expression for the reconstructed image is provided in Eq.(2).

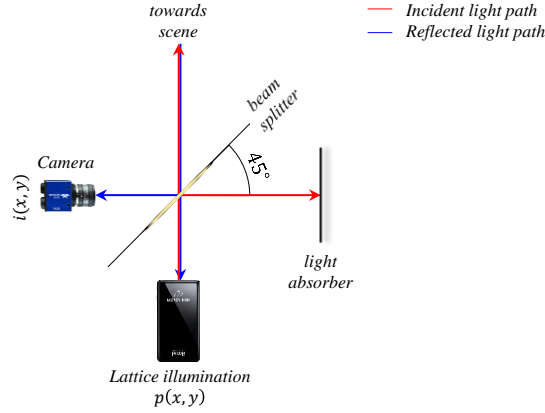


Figure 1 Apparatus used to develop the proposed super-resolution strategy

$$i_{\text{recon}}(x, y) = \iint \left(\sum_{s=0, t=0}^{P-1, Q-1} p(x - s\Delta, y - t\Delta) p(u - s\Delta, v - t\Delta) \right) r(u, v) h_{\text{cam}}(x - u, y - v; u, v) dudv \quad (2)$$

The definition of the lattice illumination pattern may be used to simplify the summation in Eq.(2), as shown below

$$i_{\text{recon}}(x, y) = \iint r(u, v) \left(\sum_{k, \ell} \text{rect}\left(\frac{x}{\Delta} - kP, \frac{y}{\Delta} - \ell Q\right) \text{rect}\left(\frac{u}{\Delta} - kP, \frac{v}{\Delta} - \ell Q\right) \right) h_{\text{cam}}(x - u, y - v; u, v) dudv \quad (3)$$

The summation in Eq.(3) may be simplified by noting that each term is different from zero only when $x - u \in (-\Delta, \Delta)$ and $y - v \in (-\Delta, \Delta)$. The simplified expression for the reconstructed image is enclosed below

$$i_{\text{recon}}(x, y) = \iint r(u, v) \left(\sum_{k, \ell} \text{rect}\left(\frac{x - u}{2\Delta} - kP, \frac{y - v}{2\Delta} - \ell Q\right) \right) h_{\text{cam}}(x - u, y - v; u, v) dudv \quad (4)$$

It is evident from Eq. (4) that the reconstructed image resembles the image acquired under the engineered PSF

$$h_{\text{engd}}(x, y; u, v) = \underbrace{\text{rect}\left(\frac{x}{2\Delta}, \frac{y}{2\Delta}\right) h_{\text{cam}}(x, y; u, v)}_{\text{central lobe}} + \underbrace{\sum_{k \neq 0, \ell \neq 0} \text{rect}\left(\frac{x}{2\Delta} - kP, \frac{y}{2\Delta} - \ell Q\right) h_{\text{cam}}(x, y; u, v)}_{\text{side lobes}} \quad (5)$$

For any field location, the side lobes in the engineered PSF may be mitigated by choosing the period $P\Delta, Q\Delta$ in excess of the worst case spot radius. In all cases, the spot size of the engineered PSF may be obtained as follows

$$\text{spot size} \left(h_{\text{engd}}(x, y; u, v) \right) = \min \left(2\Delta, 2.44 \times \frac{\lambda}{2NA_{\text{cam}}} \right) \begin{array}{l} \xrightarrow{\text{width of the rectangular pulse } \text{rect}\left(\frac{x}{2\Delta}, \frac{y}{2\Delta}\right)} \\ \xrightarrow{\text{on-axis spot size of the single-lens imager}} \end{array}$$

In the special case that $2NA_{\text{cam}}\Delta < 1.22\lambda$ one finds that the resolving power of the computational imager is uniform across the image field. The behavior is unlike a single-lens imager that exhibits severe anisotropy in resolving power.

It is worth noting that deviations from the top-hat distribution affect the shape of the engineered PSF, but leave the spot size of the computational imager unchanged.

3. Proof of concept experiment

The apparatus of Figure 2 is tasked with the objective of verifying our findings. The imager is comprised of a 25 mm double convex lens (*Edmund Optics P/N: 63-672-INK*), and a $2.2 \mu\text{m}$ pixel CMOS sensor (*Imaging Source P/N: DMK72BUC02*). The laser beam scanning (LBS) projector (*Microvision ShowWX+ P/N: AA123600-019*) is used to dispense with the need for high quality projection optics. The axial displacement between the camera and LBS projector accommodates the difference in the magnification of the camera and projector. A moving diffuser (*3M P/N: NVAG829233*) that continually slides over the resolution target minimizes the occurrence of speckle artifacts in the camera image.

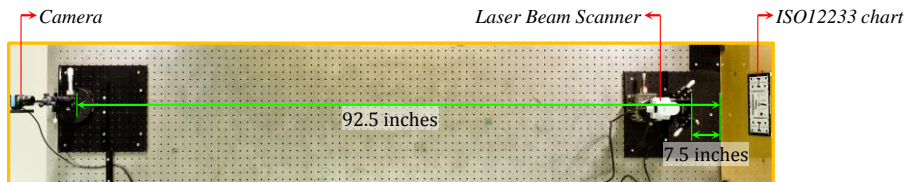


Figure 2 Apparatus used to demonstrate high quality imaging using a single-lens imager

The process of super resolution begins with the acquisition of images under integer pixel translates of the lattice illumination pattern $p(x, y) = \sum_{k=1, \ell=1}^{848, 480} \delta[\text{mod}(k, 21), \text{mod}(\ell, 21)] \text{rect}\left(\frac{x}{\Delta} - k, \frac{y}{\Delta} - \ell\right)$. A lattice spacing of 21 pixels was empirically determined to be sufficient to avoid the onset of side-lobes in the engineered PSF. The 441 (= 21 × 21) camera images acquired under lattice illumination, are resampled to accommodate the difference in the magnification of the imaging and illumination paths. The resampled camera images are multiplied with the respective illumination patterns, and the product accumulated to obtain the super resolved image.

The outcome of super resolution is made available in Figure 3. Inspection of the image insets confirms that the reconstructed image is free of ghost artifacts. Closer inspection of the red and magenta image insets indicates that the engineered imager can resolve element-4 (spatial frequency of $2 \frac{\text{cyc}}{\text{mm}}$) in the ISO12233 resolution chart. The high contrast slanted-edges in the resolution target may be used to identify the spatial frequency response (SFR) of the computational imager. It is found that the practical cutoff frequency corresponding to the 5% modulation strength remains largely unchanged over the image field. The SFR plots and experimental data will be made available for general use at <http://lyle.smu.edu/~prangara/COSI2014>.

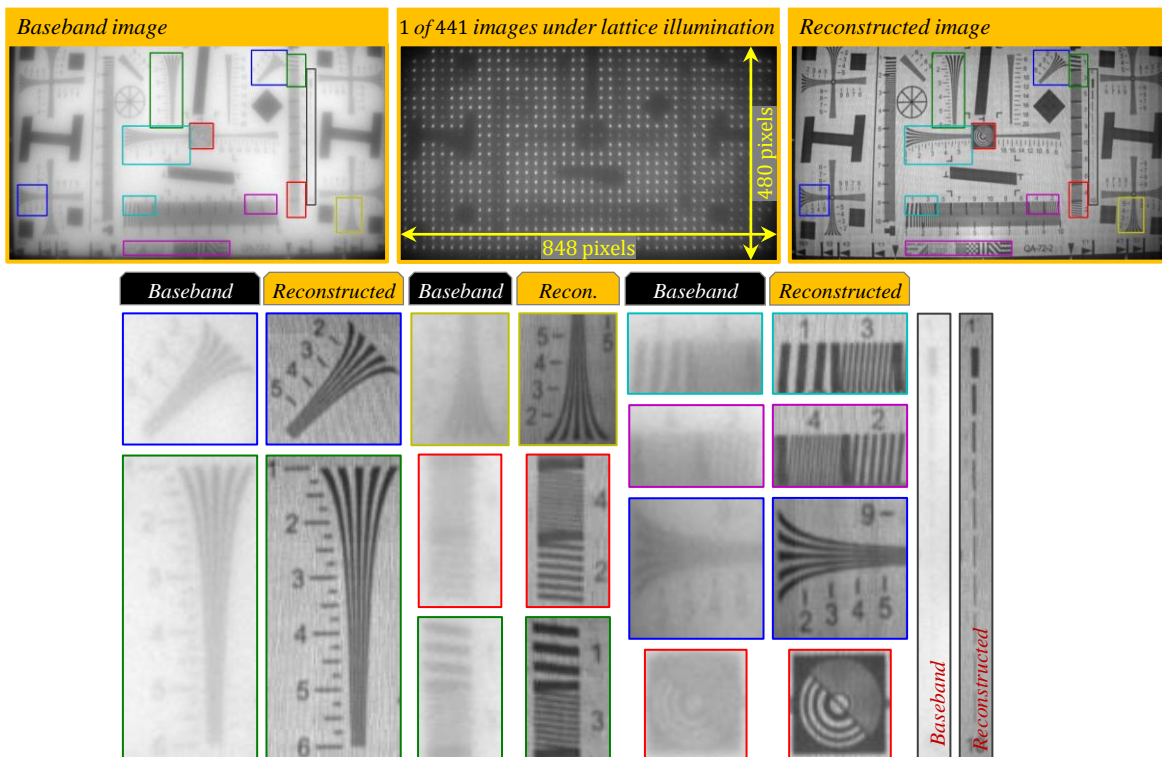


Figure 3 Super-resolving the single-lens imager in the apparatus of Figure 2

4. Closing thoughts

The strategy outlined in Section-2 and the supporting evidence in Section-3 confirm the effectiveness of lattice illumination in engineering imagers with isotropic resolving power. Preliminary analysis by the authors indicates that a broader class of illumination patterns with a compact auto-correlation function [3], may be used in lieu of lattice illumination. It is anticipated that the proposed super-resolution strategy may be used to augment the capabilities of laser based systems such as confocal microscopes, time of flight (TOF) sensors and terrestrial range scanners.

Acknowledgements

The work described in this paper was sponsored by the Army Research Laboratory and was accomplished under Cooperative Agreement Number W911NF-06-2-0035. The views and conclusions contained in this document are those of the authors and should not be interpreted as representing the official policies, either expressed or implied, of the Army Research Laboratory or the U.S. Government. The U.S. Government is authorized to reproduce and distribute reprints for Government purposes notwithstanding any copyright notation hereon.

5. References

- [1] M. Christensen, P. Rangarajan, I. Sinharoy, and P. Milojkovic, "Structured Light Optical Super-Resolution: Encoding for Limited Optical Bandwidth," in *Imaging and Applied Optics Technical Papers*, OSA Technical Digest (Optical Society of America, 2012), paper AW3B.1.
- [2] A. Lohmann and D. Paris, "Space-Variant Image Formation," *J. Opt. Soc. Am.* 55, 1007-1013 (1965).
- [3] T. Wilson, R. Juškaitis, M. Neil, and M. Kozubek, "Confocal microscopy by aperture correlation," *Opt. Lett.* 21, 1879-1881 (1996).